Acta Ciencia Indica, Vol. XLII C, No. 4, 227 (2016)

EQUILIBRIUM, KINETIC AND THERMODYNAMIC STUDY OF ADSORPTION OF NICKEL ONTO MICROWAVE ASSISTED ORANGE PEEL CARBON

N. G. TELKAPALLIWAR AND V. M. SHIVANKAR

Department of Chemistry, Dr. Ambedkar College, Deekshabhoomi, Nagpur, Maharashtra

RECEIVED : 30 December, 2016

The present study has investigated the efficiency of Microwave assisted orange peel carbon (MAOPC) for the removal of nickel from aqueous solutions. In order to understand the adsorption mechanism of nickel, the effect of pH, contact time, adsorbent dose, initial concentration of nickel and temperature of the solution has been studied. The adsorption experiments have been applied for various kinetic models such as pseudo first-order, pseudo second-order, intra particle diffusion and Elovich kinetic model. The adsorption experiments have indicates good correlation coefficient values with pseudo-second-order model. Adsorption isotherms have been studied by Lagmuir, Freundlich, Temkin and Dubinin-Radushkevich model. A correlation coefficient (R^2) value has suggested that adsorption follows Langmuir adsorption indicative of monolayer formation. Thermodynamic study revealed that adsorption of nickel by MAOPC is a chemical sorption process.

KEYWORDS : Adsorption, Orange Peel, Nickel, Isotherm, Kinetics, Thermodynamics.

INTRODUCTION

Nickel is a one of the toxic heavy metal used in silver refineries, electroplating, zinc base casting and storage battery industries [1]. The toxicity affects both human and environment. The high concentration of nickel causes cancer of lungs, nose and bone [2]. It is necessary to remove nickel from industrial wastewater before being discharged to outer water sources. There are various known advanced treatment method for the removal of nickel; such as chemical reduction, ion exchange, reverse osmosis and electro dialysis. Due to high cost of these processes use of agricultural and fruit waste materials by adsorption have been arriving with considerable attention [3].

Adsorption is inexpensive and quite attractive in terms of its efficiency of removal of pollutants from aqueous solutions. Several natural, modified and synthesized adsorbents have been used for the exclusion of heavy metals [4-12]. Agricultural and fruit waste materials contain proteins, polysaccharides and lignin with their functional groups which are responsible for metal ion adsorption [13]. The large occurrence and presence of high amount of surface functional groups make various agricultural wastes good alternatives to expensive synthetic adsorbents [14]. In recent years, many researcher widely studied removal of metal ions from

waste water by using agricultural by-products and fruit based materials. These include peat, wood, pine bark, banana pith, soybean, cottonseed hulls, peanut, shells, hazelnut shell, rice husk, sawdust, wool, orange peel, banana peel, tamarind fruit shell, bel fruit shells, corn stalk, corn cob, coir pith, hemp fibers, compost, leaves and almond husk, wheat straw and grape bagasse.[4-7, 15, 16].

Orange juice is today's one of the best widely-used beverages. Most of orange production (70%) is used to manufacture derivative products and approximately 50– 60% of the processed fruit is changed into citrus peel waste (peel, seeds and membrane residues) [17]. Orange peel is easily available and it is generally discarded as a waste. The use of orange peel as a biosorbent material presents strong potential due to its high functional group surface in the form of cellulose, pectin (galacturonic acid), hemicellulose and lignin. Hence, orange peel employed for metal ions removal from wastewater [18, 19]. Some researchers stated the use of orange peel as a precursor material for the preparation of an adsorbent by chemical modifications such as acid, alkaline, alcohol and acetone treatment [20-24]. Thus, there is a growing demand to prepared efficient, inexpensive and easily available adsorbents for the removal of heavy metals [25]. The study of this paper reports the effect of parameters such as pH, adsorbent dose, contact time, initial concentration on nickel (II) and temperature; along with the study of adsorption isotherms, adsorption kinetics and thermodynamics of removal of nickel by using orange peel.

EXPERIMENTAL

2.1. Orange Peel and Preparation of the adsorbent (MAOPC) :

Orange peels were taken from the local area of Nagpur (Maharashtra) and washed several times with distilled water to remove dust and other impurities and air dried. Then it was grinded in domestic mixer and sieved to 300 mesh size. This prepared orange peel powder was carbonized at 500^{o}C in a muffle furnace for 5 Hours. The carbonized orange peel powder was once again treated in domestic microwave (900MW) for 30 minutes in order to improve removal efficiency leading to corresponding resultant carbon which is abbreviated MAOPC.

2.2. Adsorption Experiment:

A Stock solution of 1000 mg/L of nickel ion was prepared by dissolving nickel nitrate hexahydrate [$Ni(NO_3)_2.6H_2O$] in deionised water. Batch adsorption experiments of nickel were carry out to determined the adsorption capacity of MAOPC at different nickel ion concentrations ranging from 20 to 140 mg/L. The 100 ml of nickel solutions of specified concentration of samples were shaken at 180 rpm for predetermined pH, adsorbent dose, contact time and temperature. The initial and final concentrations of the solutions were determined by Atomic Absorption spectrophotometer and the adsorption capacities of the MAOPC were calculated. When equilibrium was attained, the nickel uptake capacity for each sample was calculated according to the equation (1):

$$q_{\mathrm{e}} = \frac{(\mathrm{Co} - \mathrm{Ce})\ \mathrm{V}}{\mathrm{m}} \qquad \ldots (1)$$

where, m is the mass of adsorbent (g), V is the volume of the solution (L), C_0 is the initial concentration of metal (mg/L), C_e is the equilibrium metal concentration (mg/L) and q_e is the metal ion quantity adsorbed at equilibrium (mg/g). Adsorption experiments were carried out at different initial pH values. The initial pH of the solution was adjusted with either HCl or NaOH. The percent removal of nickel ion from the solution was calculated by the following equation (2):

$$\% \text{ Removal} = \frac{(Co - Ce)}{Co} \times 100 \quad \ldots (2)$$

where, C_0 (mg/L) is the initial metal ion concentration and C_e (mg/L) is the equilibrium metal ion concentration in the solution.

Results and discussion

3.1. Effect of pH on nickel adsorption :

Fig. 1 shows that pH is found to be sensitive for the removal efficiency of nickel ions in the aqueous solution. The result indicates that nickel removal was increased to maximum and then decreased with pH variation from 2 to 10 without altering any other parameters (adsorbent dose = 0.5 g, initial nickel concentration = 50 mg/L; contact time = 60 min, agitation speed = 180 rpm and T = 30°C). The maximum % removal of nickel was found to be 79% at pH 6. It is noted that, at pH < 3.0, H^+ ions contend with nickel ions for the surface of the adsorbent which would obstruct nickel ions from getting the binding sites of the adsorbent caused by the repulsive forces. On the other hand, the metal removal is minimum due to the improved competition of proton with nickel ions for ligand binding sites and complex formation. At pH > 6.0, the nickel ions get precipitated as nickel hydroxide. Thus, the optimal pH value was selected to be 6.0.

3.2. Effect of Contact time on nickel adsorption:

The effect of contact time on the adsorption of nickel ions by MAOPC has been studied with varying contact time from 15 to 135 min by keeping other parameters constant (pH = 6, adsorbent dose = 0.5 g, initial Ni (II) concentration = 50 mg/L, agitation speed = 180 rpm and T = 30°C). The removal of nickel ions rose rapidly with time up to 60 min and from then on increased slowly (Fig. 2). This is because of many active sites present initially for the adsorption process and they are gradually used up with time and for this reason, rate of adsorption decreases. But after 60 minutes there will be very few active sites on the adsorbent surface for the sorption process. The slowdown of removal rate shows the formation of possible monolayer of nickel ions on the outer surface and pores of the adsorbent that carry out pore diffusion onto inner surface of adsorbent. The graph indicates that, the equilibrium reached at 60 min and was taken as the optimal contact time for the later experiments.

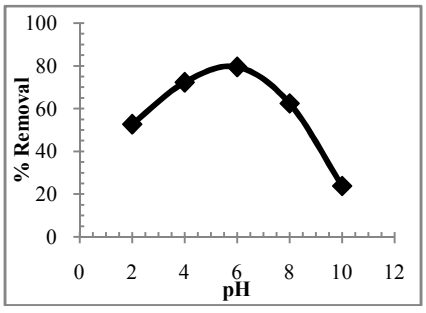

Fig 1. : Effect of pH on nickel removal capacity

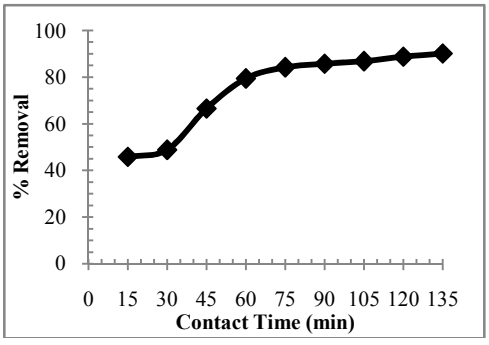

Fig 2. : Effect of contact time nickel removal capacity

3.3. Effect of adsorbent dose on nickel adsorption:

Adsorption effectiveness of nickel was studied by varying amount of adsorbents from 0.1-1 gm as usual other parameters were kept constant (pH = 6, initial nickel concentration = 50 mg/L, contact time = 60 minutes, agitation speed = 180 rpm and T = 30°C). Fig. 3 clearly shows the effect of adsorbent dose on removal of nickel for MAOPC. The removal capability of nickel was enhanced on increasing adsorbent doses. This is because of the fact that higher dose of adsorbents in the solution provides the more accessibility of exchangeable sites for the metal ions. There was no further increase in adsorption after the addition of certain amount of adsorbent (0.5 gm). It was also observed that after a certain dose of adsorbent, the equilibrium state have reached and so the amount of ions bound to the adsorbent and the amount of free ions in the aqueous solution remain constant even after addition of the dose of adsorbent. Thus, optimal adsorbent dose was selected to be 0.5 g.

3.4. Effect of temperature on nickel adsorption:

The dependence of temperature on the % removal of nickel was studied by conducting the adsorption process on to MAOPC at different temperatures within the range of 30^0C to 60^0C by keeping other parameters constant (pH = 6, adsorbent dose = 0.5 g, initial nickel concentration = 50 mg/L, contact time = 60 minutes and agitation speed = 180 rpm). It is observed that with increase in temperature from 30^0C to 60^0C the percentage removal of nickel ions was decreased from 79% to 64%. Fig. 4 indicates that the lower temperatures are in favours of extraction of nickel ion. It may be due to a propensity for the nickel ions to get away from the solid phase to the bulk phase with raise in temperature of the solution [26].

3.5. Effect of initial nickel ion concentration on adsorption:

The dependence of initial nickel ion concentration on the adsorption kinetics was studied in the rage 25 – 150 mg/L at pH 6, adsorbent dose 0.5 g, contact time 60 minutes, agitation speed 180 rpm and at a temperature 30ºC. The results obtained were plotted as percentage removal Vs concentration of nickel ion solution as shown in Fig. 5. It is observed that with increase in the initial nickel ion concentration of from 25 to 150 mg/L, the removal efficiency of metal ion decreased from 86 to 49 %. This is because of the number of active adsorption sites are not adequate to put up nickel ions. At low initial nickel ion concentration, the proportion of surface active sites to total nickel ions is high, consequently the nickel ions could act together with the adsorbent to occupy the active sites on the sorbent surface adequately.

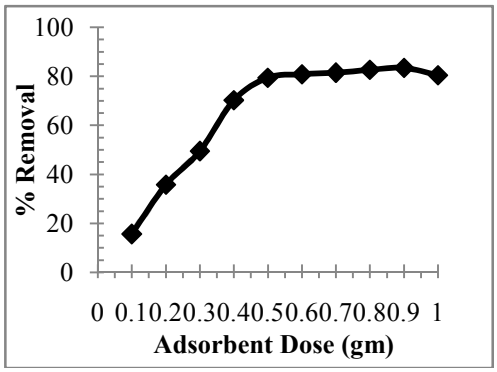

Fig. 3 : Effect of adsorbent dose on nickel removal

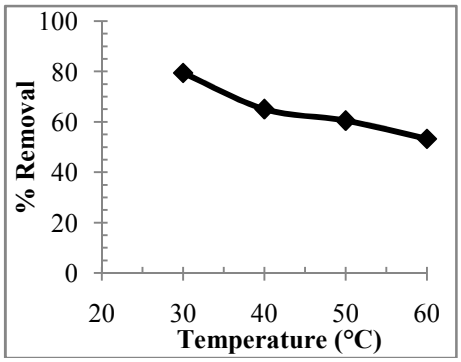

Fig. 4 : Effect of temperature on nickel removal

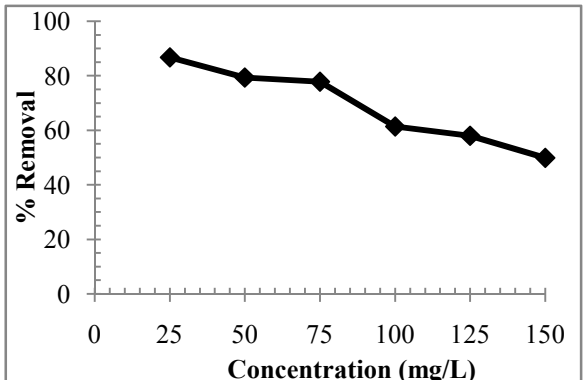

Fig. 5 : Effect of initial Ni (II) ion concentration nickel removal capacity

3.6. Adsorption Isotherms of Ni (II) onto MAOPC:

The equilibrium adsorption study of nickel removal was carried out by contacting 0.5 g of the MAOPC as adsorbent with 100 ml of diverse concentrations from 25 mg/L to 150 mg/L in 250 ml conical flasks for 60 minutes contact time. The data obtained was fitted into four well known adsorption isotherms *i.e*. Langmuir, Freundlich, Temkin and Dubinin-Radushkevich isotherm models.

3.6.1. Freundlich isotherm:

The Freundlich model [27] is a well known equation based on sorption on a heterogeneous surface. In Freundlich equation (3), q_e is the amount of nickel adsorbed by sorbent at equilibrium (mg/g), C_e is the equilibrium concentration of nickel (mg /L), K_F and n are Freundlich constants shows measure of the adsorption efficiency (mg/g) and adsorption intensity respectively.

$$q_e = K_F \, {C_e}^{1/n} \quad \ldots (3)$$

Freundlich adsorption parameters were calculated by converting the Freundlich equation (3) into its linear form.

$$ln \, q_e = lnK_F + (1/n) \ln C_e \quad \ldots (4)$$

A value of 1/n less than 1 indicates a normal Freundlich isotherm while 1/n more than 1 is suggestive of supportive adsorption [28, 29]. The Freundlich isotherm constants K_F and n were estimated from the slope and intercept from Fig. 6. The value of 1/n = 0.388 while n = 2.577 confirms that the adsorption of nickel onto MAOPC is favourable along with the R^2 value 0.923.

3.6.2. Langmuir isotherm :

Langmuir isotherm model [30] was used to estimate nickel adsorption onto MAOPC. The Langmuir isotherm is given by Eq. (5).

$$q_e = \frac{q_m K_L C_e}{1 + K_L C_e} \quad \ldots (5)$$

Converting the Langmuir equation (5) into its linear form is used to calculate parameters of Langmuir adsorption isotherm.

$$\frac{C_e}{q_e} = \frac{1}{K_L q_m} + \frac{C_e}{q_m} \quad \ldots (6)$$

where, q_m is the adsorption capacity at complete monolayer coverage (mg /g) and K_L (L/mg) is the Langmuir isotherm constant which relates to the energy of sorption. Slope and intercept of the straight line plot of C_e/q_e vs. C_e were used to calculate the values of q_m and K_L. The feasibility of the Langmuir isotherm can be expressed in terms of a dimensionless constant or separation factor, R_L of Eq. (7) where K_L is the Langmuir isotherm constant and C_0 is the initial concentration of nickel (mg/L).

$$R_L = \frac{1}{1 + K_L C_0} \quad \text{... (7)}$$

In the present study, the maximum monolayer coverage adsorption capacity (q_m) from Langmuir Isotherm model was found to be 16.94 mg/g, K_L (Langmuir isotherm constant) is 0.097 L/mg, R_L (the separation factor) is 0.291 which confirms that the equilibrium sorption was favourable and the R^2 value is 0.991 (Fig.7). This shows that adsorption isotherm data fitted well to Langmuir isotherm model.

3.6.3. Temkin Isotherm:

Temkin Isotherm contains a factor that clearly takes account of interactions among the adsorbent–adsorbate. By avoiding the particularly low and large value of concentrations, the model considers that heat of adsorption (function of temperature) of all molecules in the layer would decrease linearly rather than logarithmic coverage [31, 32]. As shown in the equation, its derivation is considered by a regular distribution of binding energies was carried out by plotting the quantity adsorbed q_e against ln C_e. The model is known by the following equation (8):

$$q_e = \frac{R\,T}{b_T} \ln (A_T\, C_e)$$

$$q_e = \frac{R\,T}{b_T} \ln (A_T) + \frac{R\,T}{b_T} \ln (C_e)$$

$$B = \frac{R\,T}{b_T}$$

$$q_e = B \ln K_T + B \ln C_e \quad \text{... (8)}$$

Where, C_e (mg/L) is equilibrium concentration of nickel, q_e (mg/g) is amount of nickel adsorbed at equilibrium, K_T (L/g) represent the Temkin isotherm equilibrium binding constant, b_T is the Temkin isotherm constant and B (J/mol) is constant related to heat of adsorption. In this study, the linear plot of q_e versus log C_e gave a straight line with the R^2 value of 0.957 (Fig. 8). Temkin constants K_T, b_T and B are calculated from the values of slope and intercept of the plot.

3.6.3 Dubinin–Radushkevich isotherm:

Dubinin–Radushkevich (D-R) isotherm is usually used to state the adsorption mechanism with a Gaussian energy allocation onto a heterogeneous surface [33, 34]. The D-R model effectively fitted high solute activities and the transitional range of concentrations data.

$$\ln q_e = \ln q_D - (K_D)\ \varepsilon^2 \quad \text{... (9)}$$

In the above D-R isotherm equation, q_e is amount of adsorbate in the adsorbent at equilibrium(mg/g); q_D is theoretical isotherm saturation capacity (mg/g); K_D is Dubinin–Radushkevich isotherm constant (mol^2/kJ^2) and ε is Dubinin–Radushkevich isotherm constant. The method was usually applied to differentiate the physical and chemical

adsorption of nickel ions with its mean free energy, E per molecule of adsorbate can be determined by the relationship [35, 36]:

$$E = \frac{1}{\sqrt{2\ K_D}} \quad \ldots (10)$$

where, K_D is D-R isotherm constant. In the meantime, the parameter ε can be designed as:

$$\varepsilon = RT \ln\left(1 + \frac{1}{C_e}\right) \quad \ldots (11)$$

where, R is gas constant (8.314 J/mol K), T is absolute temperature (K) and C_e represent adsorbate equilibrium concentration (mg/L). Dubinin-Radushkevich (D-R) isotherm model lies on the reality that it is temperature-dependent, which when adsorption data are fitted at different temperatures as a function of logarithm of amount adsorbed (ln q_e) vs ε^2 (the square of potential energy), all appropriate data will be positioned on the same curve, named as the characteristic curve [37]. From the linear plot of D-R model (Fig. 9), q_D was found to 12.589 mg/g, the mean free energy (E) = 0.199 KJ/mol and R^2 = 0.855 slightly lower than that of Tempkin model.

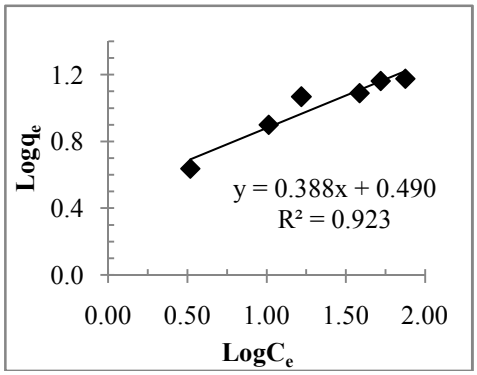

Fig. 6 : Freundlich model for nickel sorption

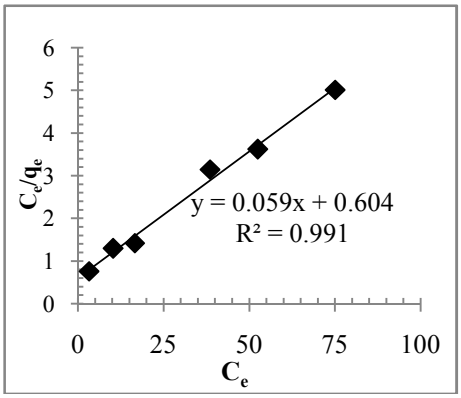

Fig. 7 : Langmuir model for nickel sorption

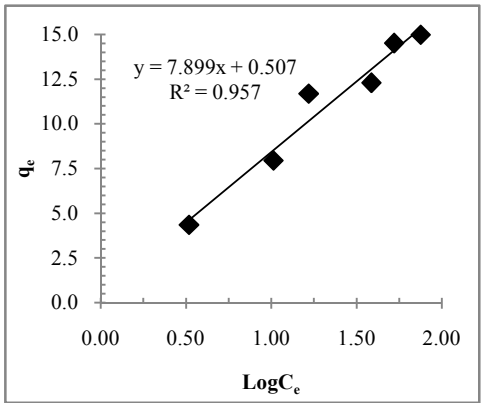

Fig. 8 : Temkin model for nickel sorption

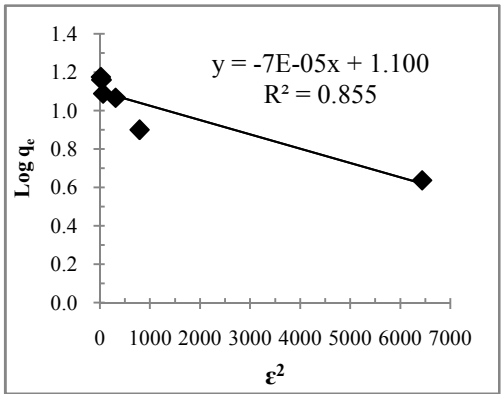

Fig. 9 : D-R model for nickel sorption

Langmuir, Freundlich, Temkin and Dubinin-Radushkevich adsorption isotherms for removal of nickel from aqueous solution onto MAOPC are described in Fig. 6, 7, 8, and 9. It established that the experimental information fitted well to all these isotherm models. Correlation coefficients values indicated that Langmuir isotherm gives a good model for the

adsorption system, which is based on monolayer sorption on to the surface limiting finite number of identical sorption sites. The values of various constants of isotherm models were determined and were represented in the Table-1.

Table 1. Langmuir, Freundlich, Temkin and Dubinin-Radushkevich Isotherm parameters of nickel sorption on MAOPC

Isotherm	Parameters	
Langmuir Isotherm	q_m (mg/g)	16.94
	K_L (L/mg)	0.097
	R_L	0.291
	R^2	0.991
Freundlich Isotherm	K_F (mg/g)	3.09
	$1/n$	0.388
	N	2.577
	R^2	0.923
Temkin Isotherm	K_T (L/mg)	1.159
	B (J)	3.429
	b_T	734.65
	R^2	0.957
Dubinin-Radushkevich Isotherm	q_D (mg/g)	12.59
	K_D (mol^2/kJ^2)	1.6 x 10^{-4}
	E (KJ/mol)	0.0559
	R^2	0.855

3.7. Adsorption Kinetic Study:

The kinetic study of adsorption of metal ions from aqueous solutions plays an important role because it demonstrates important insight into the reaction pathways and mechanism of the adsorption process. The rate and kinetics of adsorption of nickel on to the MAOPC was studied with pseudo first-order model, pseudo second-order model, Intra-particle diffusion model and Elovich kinetic model.

3.7.1. Pseudo first-order kinetic model:

The pseudo first-order kinetic model [38] has been extensively used to understand the metal adsorption kinetics. The pseudo first-order kinetic model is given by equation (12),

$$\frac{dq}{dt} = k_1 + (q_e - q_t) \quad \ldots (12)$$

where k_1 (min^{-1}) is the rate constant of the pseudo first-order adsorption, q_t (mg/g) represent the amount of adsorption at time t (min) and q_e (mg/g) is the amount of adsorption at equilibrium. By applying boundary conditions q_t =0 at t = 0 and $q_t = q_t$ at $t = t$, the integrated form of equation (12) becomes,

$$log(q_e - q_t) = \log q_e - \left(\frac{k_1}{2.303}\right) t \quad \ldots (13)$$

The sorption rate can be estimated by plotting *log* $(q_e - q_t)$ versus *t.* Linear kinetics plot were obtained that can be clearly seen in Fig 10 with excellent correlation coefficient

(R^2 = 0.977), which shows that pseudo first-order kinetic model is suitable to the nickel adsorption onto MAOPC. The nickel adsorption was found with the rate constants $k_1 = 3.22 \times 10^{-3}$ min^{-1}. The amount of nickel adsorbed (q_e) was estimated and it was found to be 9.01 mg/g.

3.7.2. Pseudo second-order kinetics model:

Ho's pseudo second-order kinetics [38] was used to analyze the adsorption kinetic data. This is represented by,

$$\frac{dq}{dt} = k_2 \, (q_e - q_t)^2 \qquad \text{... (14)}$$

By applying boundary conditions $q_t = 0$ at $t = 0$ and $q_t = q_t$ at $t = t$, integrated form of equation (14) becomes,

$$\left(\frac{t}{q_t}\right) = \left(\frac{1}{k_2 \, {q_e}^2}\right) + \left(\frac{1}{q_e}\right) \, t \qquad \text{... (15)}$$

where k_2 (g/mg. min) symbolise the rate constant of the pseudo-second-order adsorption, q_t (mg/g) represents the amount of adsorption at time t (min) , q_e (mg/g) stand for the amount of adsorption at equilibrium and initial sorption rate , h stand for $k_2 q_e^2$ (mg/g min). Plot of t/q_t versus t, gives the parameters of pseudo second-order kinetics model. From Fig. 11, the values of q_e, k_2, h and correlation coefficient (R^2) was found to be 10.98 mg/g, 3.41 × 10^{-3} g mg^{-1} min^{-1}, 1.047 mg g^{-1} min^{-1} and 0.985 respectively.

3.7.3. Intra-particle diffusion model:

Intra-particle diffusion kinetic model was proposed by Weber and Moris [39–41] for the diffusion controlled sorption process. The intra-particle diffusion equation is given by Eq. (16),

$$q_t \; = \; k_d \, t^{1/2} \; + \; C \qquad \text{... (16)}$$

where, k_d is the intra-particle rate constant (mg g^{-1} min$^{-0.5}$). Plot of q_t versus $t^{0.5}$ was determined the values of the intra-particle rate constant and constant C (mg g^{-1}) that gives an idea about the thickness of the boundary layer, *i.e.*, the higher the value of C, greater is the boundary layer effect. Fig. 12 suggested that two different types of mechanisms are mixed up in the adsorption process. The preliminary curve represents the boundary layer effect while the linear part relates to intra-particle diffusion. The high correlation coefficient (R^2) value (Table 2) indicates the probability of the sorption process being inhibited by both the particle and the pore diffusion models [42–43].

3.7.4. Elovich kinetic model :

Elovich kinetic model [44] is the useful kinetic models for describing sorption process. The Elovich equation is known by Eq. (17) where A is the initial sorption rate (mg g^{-1} min^{-1}) and B is the constant of desorption (g mg^{-1}) for adsorption experiment. Eq. (18) is the simplified appearance of Elovich kinetic equation [45].

$$dq_t = A \, e^{(-Bqt)} \qquad \text{... (17)}$$

$$q_t \; = \; \left(\frac{1}{B}\right) \, ln \, AB \; + \; \left(\frac{1}{B}\right) \, ln \, t \qquad \text{... (18)}$$

The plot of q_t against lnt (Fig. 13) gives a slope 1/B, which shows the number of available sites to put up nickel ions. From the information of available sites, the adsorption behaviour of the adsorbent is designed which eventually validates that chemisorption step is rate

determined [46]. The correlation coefficient (R^2) values from Table 2 validated the appropriateness of this model.

The validity of the above kinetic models for the removal of nickel onto MAOPC was observed in the subsequent order as pseudo second-order > pseudo-first-order > Elovich > Intra-particle diffusion. The reported correlation coefficients (R^2) value indicates that the adsorption experimental results shows better fit to pseudo second order kinetic model. The values of different constants of kinetic models were calculated and were presented in the Table-2.

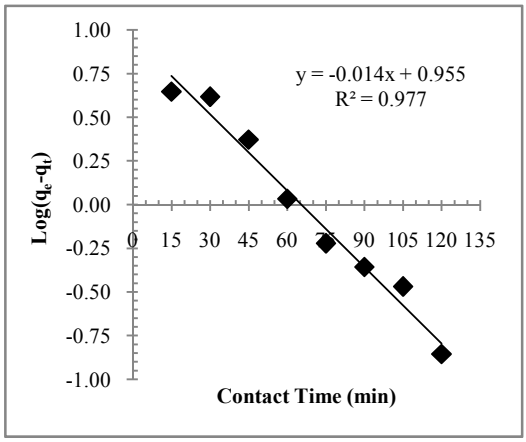

Fig. 10 : Pseudo first order model

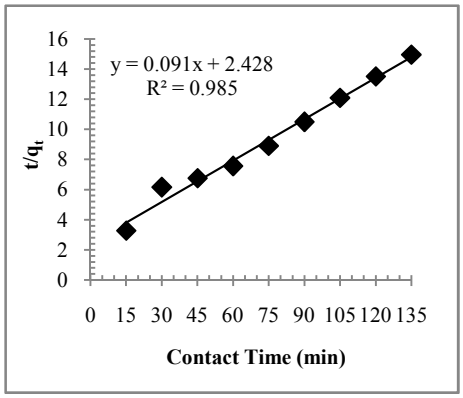

Fig. 11 : Pseudo second order model

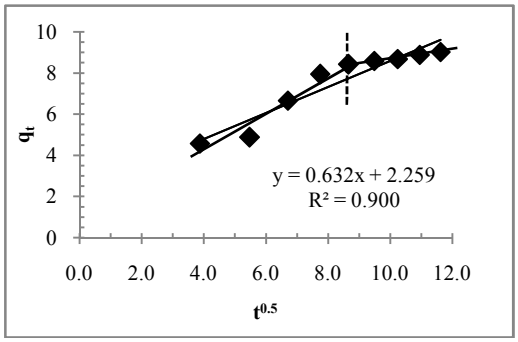

Fig. 12 : Intra-particle diffusion model

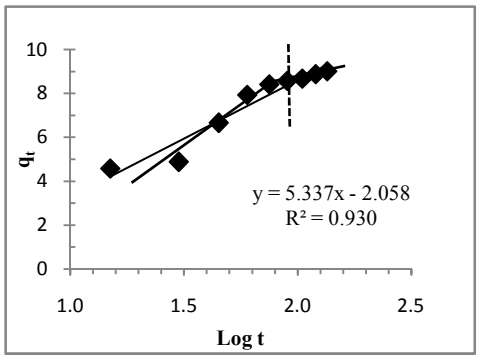

Fig. 13 : Elovich kinetic model

3.8. Thermodynamic Parameters:

Thermodynamic study is much more useful as it provides effective information on carrying out adsorption. To find out thermodynamic parameters of nickel adsorption onto MAOPC study was carried at four different temperatures *i.e.* 303, 313, 323, 333 K. This helpful study was done to see the consequence of temperature on nickel adsorption onto MAOPC, thermodynamic parameters related with adsorption method, such as standard free energy change ($\Delta G°$), standard enthalpy change ($\Delta H°$) and standard entropy change ($\Delta S°$)) were determined by using the following equations (19, 20 and 21) [47].

$$\Delta G^o = -R\,T\,\ln K \quad \ldots (19)$$

$$\Delta G^o = \Delta H^o + T\,\Delta S^o \quad \ldots (20)$$

$$\ln K = \frac{\Delta S^{o}}{R} - \frac{\Delta H^{o}}{RT} \quad \ldots (21)$$

where K_c is adsorption equilibrium constant; R is Universal gas constant (8.314 J mol^{-1} K^{-1}) and T is Temperature in Kelvin.

Table 2. Kinetics parameters of the different kinetic models for adsorption of Ni (II).

Kinetic Model	Parameters	
Pseudo first-order model	q_e (mg/g))	9.01
	k_1 (min^{-1})	3.22×10^{-3}
	R^2	0.977
Pseudo second-order model	q_e (mg/g)	10.98
	k_2 (g mg^{-1} min^{-1})	3.41×10^{-3}
	h (mg g^{-1} min^{-1})	1.047
	R^2	0.985
Intra-particle diffusion model	k_d (g mg^{-1} $min^{-0.5}$)	0.632
	C	2.259
	R^2	0.9
Elovich kinetic model	A (mg g^{-1} min^{-1})	9.537
	B (g mg^{-1})	0.431
	R^2	0.930

The values of $\Delta S°$ and $\Delta H°$ can be determined from intercept and slope of linear plot of log K against $1/T$ (Fig 14). The calculated values of $\Delta G°$, $\Delta H°$, and $\Delta S°$ are shown in Table 3. The values of ΔG^0 lies in between 0.655 to 4.101 kJ/mol at all temperatures confirm that the nickel adsorption is a chemical sorption process. The negative value of ΔH^0 represents an exothermic adsorption process and negative value of ΔS^0 indicates the decrease in randomness at the solid-solution interface during sorption process [48].

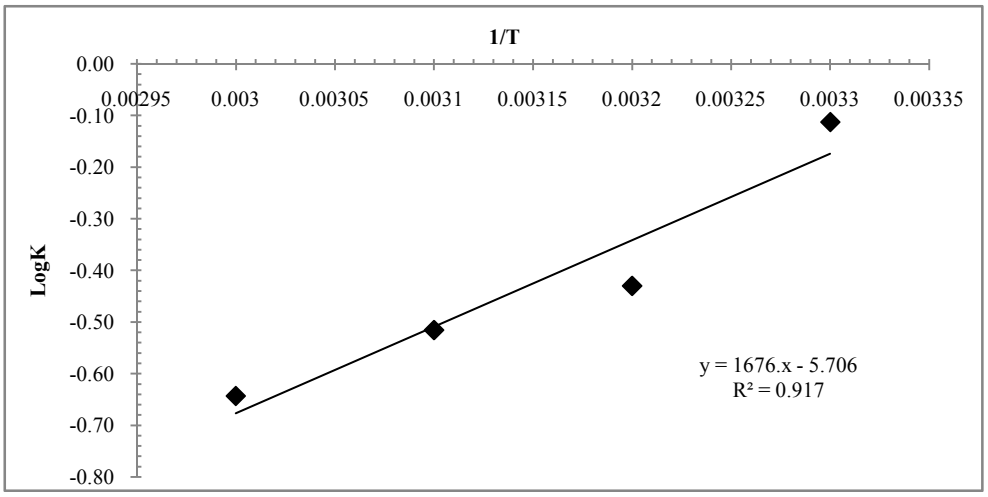

Fig. 14. The plot of log *K* vs. 1/*T*

Table 3. Thermodynamic parameters of adsorption of nickel oto MAOPC

T (K)	ΔG (kJ/mole)	ΔH (kJ/mole)	ΔS (kJ mol^{-1} K^{1})
303	0.655		
313	2.577	– 32.09	– 0.109
323	3.188		
333	4.101		

Conclusion

Present paper reported the efficiency and applications of microwave assisted orange peel carbon (MAOPC), one of the modified inexpensive easily available adsorbent for the removal of nickel from aqueous solution. The investigation of effect of initial pH, initial nickel ion concentration, contact time, temperature and adsorbent dose on the removal capacity of nickel by MAOPC indicates the dependency on these parameters. Quantitative adsorption equilibrium study of removal of nickel onto MAOPC from aqueous solution confirms the validity of obtained results and the adsorption data are well fitted for the Langmuir adsorption isotherm model. The kinetic data obtained for adsorption of nickel on MAOPC followed the pseudo second-order kinetic model with good correlation coefficient value. Thermodynamic study of sorption of nickel using MAOPC revealed that it is a chemical sorption process.

Acknowledgement

The authors thank the Principal of Dr. Ambedkar College, Deekshabhoomi, Nagpur for encouragement and providing necessary facilities in the Department of Chemistry.

References

1. Kadirvelu, K., Thamaraiselvi, K., Namasivayam, C., *Sep. Pur. Technol*., **24**, 497 (2001).
2. Hasar, H., *J. Hazard. Mater.,* **B97**, 49–57 (2003).
3. Hasar, H., Cuci, Y., Anadolu Univ*., J. Sci. Technol.,* **1**, 201 (2000).
4. Ibrahim, M.N.M., Ngah, W.S.W., Norliyana, M.S., Daud, W.R.W., Rafatullah, M., Sulaiman, O., Hashim, R., *J. Hazard. Mater*., **182**, 377–385 (2010).
5. Teoh, Y.P., Khan, M.A., Choong, T.S.Y., *Chemical Engineering Journal*, **217**, 248–255 (2013).
6. George, Z., Kyzas, Margaritis Kostoglou, *Materials.* **7**, 333-364 (2014).
7. Gupta, V. K., Carrott, P. J.M., Ribeiro Carrott, M.M.L. and Suhas, *Critical Reviews in Environmental Science and Technology*, **39 : 10**, 783-842 (2009).
8. Lalhruaitluanga, H., Jayaram, K., Prasad, M.N.V., Kumar, K.K., *J. Hazard. Mater.,* **175,** 311–318 (2010).
9. Liao, S.W., Lin, C.I., Wang, L.H., *Journal of the Taiwan Institute of Chemical Engineers,* **42**, 166–172 (2011).
10. Depci, T., Kul, A.R., Önal, Y*., Chemical Engineering Journal,* **200**, 224–236 (2012).
11. Mouni, L., Merabet, D., Bouzaza, A., Belkhiri, L., *Desalination,* **276**, 148–153 (2011).
12. Azouaou, N., Belmedani, M., Mokaddem, H., Sadaoui, Z., *Chemical Engineering Transactions,* **32**, 55-60 (2013).
13. Wase, J., Forster, C., *Taylor & Francis Ltd*. (1997).
14. Bulut. Y., Tez, Z., *J. Hazard. Mater.,* **149**, 35–41 (2007).
15. Sivasankar, V., Rajkumar, S., Murugesh, S., Darchen, A., *J. Hazard. Mater.,* **225–226**, 164–172 (2012).

16. Malik, D. S., Jain, C. K., Yadav, Anuj K., *Applied Water Science*, **1-24**, DOI: 10.1007/s13201-016-0401-8 (2016).
17. Wilkins, M.R., Suryawati, L., Maness, N.O., Chrz, D., *World J. Microbiol. Biotechnol.,* **23**, 1161-1168 (2007a).
18. Wan Ngah, W.S., Hanafiah, M., *Bioresour Technol.,* **99**, 3935–3948 (2007).
19. Rao, Ajmal M., Ahmad, R.A.K.R., Ahmad, J., *J. Hazard. Mater.,* **B79**, 117–131 (2000).
20. Perez Marín, A.B., Aguilar, M.I., Meseguer, V.F., Ortũno, J.F., Loŕens, M., Śaez, J., *Chem. Eng. J.,* **155**, 199–206 (2008).
21. Li, X., Tang, Y., Xuan, Z., Liu, Y., Luo, F., *Sep. Purif. Technol.,* **55**, 69–75 (2007).
22. Biswas, B.K., Inoue, K., Ghimire, K.N., Ohta, S., Harada, H., Ohto, K., Kawakita, H., *J. Colloid Interface Sci.,* **312**, 214–223 (2007).
23. Liang, S., Guo, X., Feng, N., Tian, Q., *Colloids Surf. B: Biointerfaces,* **73**, 10–14 (2009).
24. Liang, S., Guo, X., Feng, N., Tian, Q., *J. Hazard. Mater.*, **170**, 425–429 (2009).
25. Anirudhan, T.S., Sreekumari, S.S., *J. of Environmental Sciences,* **23**, 12, 1989–1998 (2011).
26. Chen, C., Yang, C., Chen, C., Chen, W., *J. Hazard. Mater.,* **163**, 1068-1075 (2009).
27. Freundlich, H.M.F., *Z. Phys. Chem.,* **57A,** 385–470 (1906).
28. Haghseresht, F., La, G., *Energy Fuels*., **12**, 1100–1107 (1998).
29. Fytianos, K., Vondrias, F., Kokkalis, F., *Chemosphere,* **40**, 3–6 (2000).
30. Langmuir, I., The constitution and fundamental properties of solids and liquids, *J. Am. Chem. Soc*., **38**, 2221–2295 (1916).
31. Temkin, M.J., Pyzhev, V., Recent modifications to Langmuir isotherms, *Acta Physiochim*, USSR, **12**, 217–222 (1940).
32. Aharoni, C., Ungarish, M., Kinetics of activated chemisorptions, Part 2, Theoretical models, *J. Chem. Soc. Faraday Trans*., **73**, 456–464 (1977).
33. Gunay, A., Arslankaya, E., Tosun, I., *J. Hazard. Mater.,* **146**, 362–371 (2007).
34. Dabrowski, A., *Adv. Colloid Interface Sci.,* **93**, 135–224 (2001).
35. Dubinin, M.M., *Chem. Rev*., **60**, 235–266 (1960).
36. Hobson, J.P., *J. Phys. Chem.,* **73**, 2720–2727 (1969).
37. Foo, K.Y., Hameed, B.H., *Chemical Engineering Journal,* **156**, 2–10 (2010).
38. Ho, Y.S. and Mckay, G., *Resour. Conserv. Recycl*., **25**, 171–193 (1999 a).
39. Weber, W.J., Morris, J.C., *J. Sanitary Eng. Div.,* **90**, 79–107 (1964).
40. Chanda, M., O'Driscoll, K.F., Rempel, G.L., *React. Polym.,* **1**, 281–293 (1983).
41. Poots, V.J.P., McCay, G., *J. Chem. Technol. Biotechnol.,* **30**, 279–292 (1980).
42. Mahramanlioglu, M., Kizilcikli, I., Bicer, I.O., *J. Fluorine Chem.,* **115**, 41–47 (2002).
43. Kalavathy, M.H., Karthikeyan, T., Rajagopal, S., Miranda, L.R., *J. Colloid Interface Sci*., **292**, 354–362 (2005).
44. Aharoni, C., Tompkins, F.C., *Advance in Catalysis and Related Subjects*, Academic Press, New York (1970).
45. Chien, S.H., Clayton, W.R., *Soil Sci. Soc. Am. J.,* **44**, 265–268 (1980).
46. Juang, R.S., Chen, M.L., *Ind. Eng. Chem. Res.,* **36**, 813–820 (1997).
47. Telkapalliwar, N. G., Shivankar, V. M., *International Journal of Application or Innovation in Engineering & Management,* **5**, 4, 76-82 (2016).
48. Aksu, Z., İşoğlu, A., *Process Biochemistry*, **40**, 9, 3031–3044 (2005).

❑